The Interplay Between Feedback and Buffering in Homeostasis: Supplementary Information 2

S2 Regulation of Glycolysis

This supplementary section introduces a minimal model for glycolysis, analyzes the model, and uses the qualitative results to find new relationships in existing experimental data.

In this section we examine the regulation of glycolysis. In particular, we look at the effects of glycolytic feedback and creatine phosphate buffering on the stability and regulation of ATP concentrations. We then use this analysis to compare the regulation of ATP by different species.

The minimal models of glycolysis that we analyze here are built on models found in existing literature that do not include buffering [3]. Initially, we look at the case where buffering is rapid (S2.1), then analyze more general cases of buffering (S2.2), followed by cases where more general feedback structures are allowed (S2.3). As in [3], we assume that the total concentration of adenosine phosphates in the cell (ATP + adenosine diphosphate (ADP) + adenosine monophosphate (AMP)) remains constant, and that the activating effects of AMP can be modelled as ATP inhibition. By further assuming total creatine (Cr + pCr) to be constant, we simplify the buffering reaction as pCr $\leftrightarrow$ ATP.

Consider

$$\begin{aligned} \dot{m} &= \underbrace{f(y)}_{\text{PFK}} - \underbrace{w(y)m}_{\text{PK}} \\ \dot{y} &= -q\underbrace{f(y)}_{\text{PFK}} + (q+1)\underbrace{w(y)m}_{\text{PK}} - \underbrace{g_y(y,x) + g_x(x,y)}_{\text{Buffering}} - \underbrace{V_y(1+d_y)}_{\text{ATP Demand}} \\ \dot{x} &= \underbrace{g_y(y,x) - g_x(x,y)}_{\text{Buffering}}, \end{aligned} \tag{1}$$

where y represents ATP concentration, x represents pCr concentration (for vertebrates), and m is a lumped variable representing intermediate metabolites (see also Figure S2.1). Also, $g_y(y,x)$ and $g_x(x,y)$ are the reaction rates for the ATP $\leftrightarrow$ pCr reaction, the constant V_y is the nominal ATP demand, and q is the stoichiometric investment/return ratio for the autocatalysis of ATP.

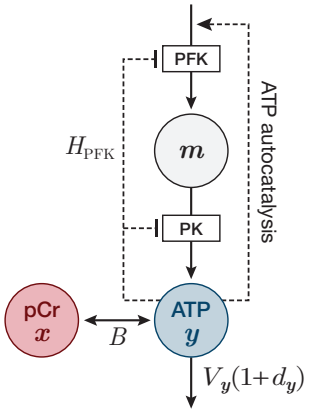


Figure S2.1: **Glycolytic Feedback and Creatine Phosphate Buffering of ATP** Network diagram for a minimal model describing ATP production by glycolysis and ATP buffering by pCr. The primary feedback gain, H_{PFK}, in this model is represented by the (negative) slope of ATP concentration to PFK activity. Here, m represents intermediate metabolites in glycolysis.

The reaction rates can, for example, be modelled by Hill functions, such that

$$\begin{aligned} f(y) &= \frac{V_{\mathrm{PFK}} y^a}{1+\gamma_h y^h}\,, \quad w(y) = \frac{V_{\mathrm{PK}}}{1+\gamma_g y^g}\,, \\ g_y(y,x) &= \frac{b_y y}{1+\frac{y}{K_y}+\frac{x}{K_x}}\,, \quad g_x(x,y) = \frac{b_x x}{1+\frac{y}{K_y}+\frac{x}{K_x}}\,, \end{aligned} \tag{2}$$

where V_{PFK}, γ_h, h, and a are parameters describing the reaction rate of phosphofructo kinase (PFK), and V_{PK}, γ_g, g are the parameters describing the reaction rate of pyruvate kinase (PK). The parameters b_y, b_x, K_y and K_x describe the reaction rates of creatine kinase, and are also dependent upon creatine and ADP concentrations.

The steady-state solution of Equation (1) is

$$\begin{aligned} w(\bar{y})\bar{m} &= f(\bar{y}) = V_y \\ \bar{y} &= \bar{B}\bar{x}\,, \end{aligned}$$

where $\bar{B}$ is the steady-state ratio between ATP and pCr, such that $g_y(\bar{B}\bar{x},\bar{x}) = g_x(\bar{x},\bar{B}\bar{x})$.

S2.1 Regulation of Buffered Glycolysis with Rapid Buffering

The following section analyzes a (further simplified) minimal model for glycolysis, determining the critical feedback gain for which its steady state is stable. The stability analysis is carried out by linearizing the system about its steady state, followed by eigenvalue analysis of the linear system. The critical feedback gain is then used to determine a limit on the effectiveness of steady-state regulation.

We first look at the case where buffering is rapid. Linearizing Equation (1) about the nominal steady state with deviations $\Delta y = y - \bar{y}$, $\Delta m = m - \bar{m}$, and $\Delta x = x - \bar{x}$, results in

$$\begin{aligned} \Delta\dot{m} &= -w(\bar{y})\Delta m + (\alpha_f - \alpha_w\bar{m})\Delta y \\ \Delta\dot{y} &= (q+1)w(\bar{y})\Delta m - (q\alpha_f - (q+1)\alpha_w\bar{m})\Delta y - \alpha_y\Delta y + \alpha_x\Delta x - V_y d_y \\ \Delta\dot{x} &= \alpha_y\Delta y - \alpha_x\Delta x\,, \end{aligned} \tag{3}$$

where

$$\alpha_y = \frac{\partial}{\partial y}[g_y - g_x]\,, \quad \alpha_x = \frac{\partial}{\partial x}[g_x - g_y]\,,$$
$$\alpha_f = \frac{\partial f}{\partial y}(\bar{y})\,, \quad \alpha_w = \frac{\partial w}{\partial y}(\bar{y})\,.$$

The buffering equilibrium ratio is

$$B = \frac{\alpha_y}{\alpha_x}\,.$$

For the rapid case, we can determine a reduced model similar to that used in SI1.3. By assuming rapid equilibrium, $\Delta x = B\Delta y$, and that the total concentration $\Delta y_T = \Delta y + \Delta x$ is a slow variable, the model in Equation (3) reduces to

$$\begin{aligned} \Delta\dot{m} &= -w(\bar{y})\Delta m + (\alpha_f - \alpha_w r\bar{m})\Delta y \\ (1+B)\Delta\dot{y} &= (q+1)w(\bar{y})\Delta m - (q\alpha_f - (q+1)\alpha_w r\bar{m})\Delta y - V_y d_y\,. \end{aligned} \tag{4}$$

We next non-dimensionalize the system, resulting in

$$\begin{aligned} \Delta\dot{m}_n &= -w(\bar{y})\Delta m_n + (\alpha_f - \alpha_w r\bar{m})\frac{\bar{y}}{V_y}\Delta y_n \\ \Delta\dot{y}_n &= \frac{1}{1+B}(q+1)w(\bar{y})\frac{V_y}{\bar{y}}\Delta m_n - \frac{1}{1+B}(q\alpha_f - (q+1)\alpha_w r\bar{m})\Delta y_n - \frac{V_y}{\bar{y}}\frac{1}{1+B}d_y\,, \end{aligned} \tag{5}$$

where

$$\Delta m_n = \frac{\Delta m}{V_y} \quad \text{and} \quad \Delta y_n = \frac{\Delta y}{\bar{y}}\,.$$

Equation (5) can be rewritten as

$$\begin{pmatrix} \Delta\dot{m}_n \\ \Delta\dot{y}_n \end{pmatrix} = A_1 \begin{pmatrix} \Delta m_n \\ \Delta y_n \end{pmatrix} + A_2 d_y\,,$$

where

$$A_1 = \begin{pmatrix} -w(\bar{y}) & (\alpha_f - \alpha_w r\bar{m})\frac{\bar{y}}{V_y} \\ \frac{1}{1+B}(q+1)w(\bar{y})\frac{V_y}{\bar{y}} & -\frac{1}{1+B}(q\alpha_f - (q+1)\alpha_w r\bar{m}) \end{pmatrix} \quad \text{and} \quad A_2 = \begin{pmatrix} 0 \\ -\frac{V_y}{\bar{y}}\frac{1}{1+B} \end{pmatrix}.$$

For stability we require the trace $\mathrm{Tr}(A_1) < 0$ and determinant $\mathrm{Det}(A_1) > 0$, such that

$$\begin{aligned} &-w(\bar{y}) - \frac{1}{1+B}(q\alpha_f - (q+1)\alpha_w r\bar{m}) < 0 \quad \text{and} \\ &(q\alpha_f - (q+1)\alpha_w r\bar{m})\frac{1}{1+B}w(\bar{y}) - (\alpha_f - \alpha_w r\bar{m})(q+1)\frac{1}{1+B}w(\bar{y}) > 0\,, \end{aligned}$$

which simplifies to

$$-q\alpha_f < (1+B)w(\bar{y}) - (q+1)\alpha_w r\bar{m} \quad \text{and} \quad -\alpha_f > 0\,. \tag{6}$$

In non-dimensionalized form, this can be rewritten as a constraint on feedback gain:

$$0 < H_{\mathrm{PFK}} < H_{\mathrm{crit}}\,, \tag{7}$$

where

$$H_{\text{crit}} = \frac{(1+B)\kappa + (q+1)H_{\text{PK}}}{q}$$
$$H_{\text{PFK}} = -\alpha_f \frac{\bar{y}}{V_y} = -\frac{\partial f}{\partial y}(\bar{y})\frac{\bar{y}}{f(\bar{y})}$$
$$H_{\text{PK}} = -\alpha_w \bar{m}\frac{\bar{y}}{V_y} = -\frac{\partial w}{\partial y}(\bar{y})\frac{\bar{y}}{w(\bar{y})}\,,$$

$\kappa = \bar{y}/\bar{m}$, and the buffering equilibrium ratio in terms of the quasi-steady state is

$$B = \frac{\Delta x}{\Delta y}\,.$$

The steady-state regulation is lower bounded by

$$\phi_{\text{ss}} = \left\| \frac{\Delta \bar{y}_n}{\bar{d}_y} \right\| = \frac{1}{H_{\text{PFK}}} > \frac{1}{H_{\text{crit}}} = \frac{q}{(1+B)\kappa + (q+1)H_{\text{PK}}}\,.$$

When the reaction rates are modelled by the Hill functions in Equation (2), we have

$$H_{\text{PFK}} = h\frac{\gamma_h \bar{y}^h}{1+\gamma_h \bar{y}^h} - a \quad \text{and} \quad H_{\text{PK}} = g\frac{\gamma_g \bar{y}^g}{1+\gamma_g \bar{y}^g}\,.$$

S2.2 Regulation of Buffered Glycolysis for General Buffering

The following section carries out further analysis of a minimal model of glycolysis. The analysis is similar to Section S2.1, but with a higher-order model to represent non-rapid buffering.

We next study stability constraints for the general buffering case. For simplicity, we first determine stability conditions before non-dimensionalizing. For the non-rapid case, Equation (3) can be rewritten as

$$\begin{bmatrix} \Delta\dot{m} \\ \Delta\dot{y} \\ \Delta\dot{x} \end{bmatrix} = A \begin{bmatrix} \Delta m \\ \Delta y \\ \Delta x \end{bmatrix} - \begin{bmatrix} 0 \\ V_y \\ 0 \end{bmatrix} d_y\,,$$

where

$$A = \begin{bmatrix} -w & \alpha_f - \alpha_w \bar{m} & 0 \\ (q+1)w & -(q\alpha_f - (q+1)\alpha_w \bar{m} + \alpha_y) & \alpha_x \\ 0 & \alpha_y & -\alpha_x \end{bmatrix}.$$

A matrix of the form

$$\begin{bmatrix} a & b & 0 \\ c & d & e \\ 0 & f & g \end{bmatrix}$$

has the characteristic polynomial

$$s^3 - (a+d+g)s^2 + (ad+dg+ag-ef-bc)s + (-adg+aef+bcg) = 0\,.$$

Stability requires that

$$\begin{aligned} &\alpha \equiv -(a+d+g) > 0 \\ &\beta \equiv ad+dg+ag-ef-bc > 0 \\ &\gamma \equiv -adg+aef+bcg > 0 \\ &\alpha\beta > \gamma\,. \end{aligned} \tag{8}$$

Therefore, for the buffering model, stability requires that

$$\begin{aligned}
\alpha &\equiv w + q\alpha_f - (q+1)\alpha_w\bar{m} + \alpha_y + \alpha_x > 0 \\
\beta &\equiv (w+\alpha_x)(q\alpha_f - (q+1)\alpha_w\bar{m} + \alpha_y) + w\alpha_x - \alpha_x\alpha_y - (\alpha_f - \alpha_w\bar{m})(q+1)w(\bar{y}) \\
&= -w\alpha_f + q\alpha_x\alpha_f + w(\alpha_x+\alpha_y) - (q+1)\alpha_x\alpha_w\bar{m} > 0 \\
\gamma &\equiv w\alpha_x(q\alpha_f - (q+1)\alpha_w\bar{m} + \alpha_y) - w\alpha_x\alpha_y - (\alpha_f - \alpha_w\bar{m})(q+1)w\alpha_x \\
&= -w\alpha_x\alpha_f > 0\,,
\end{aligned}$$

and, from $\alpha\beta > \gamma$, that

$$[w + q\alpha_f - (q+1)\alpha_w\bar{m} + \alpha_y + \alpha_x][-w\alpha_f + q\alpha_x\alpha_f + w(\alpha_x+\alpha_y) - (q+1)\alpha_x\alpha_w\bar{m}] > -w\alpha_x\alpha_f\,.$$

When non-dimensionalized, the stability conditions can be written as

$$\begin{aligned}
H_{\mathrm{PFK}} &< \frac{\kappa + H_{\mathrm{PK}}(q+1) + \eta_x(1+B)}{q} \\
H_{\mathrm{PFK}} &< \frac{(1+B)\kappa + H_{\mathrm{PK}}(q+1)}{q - \frac{\kappa}{\eta_x}} \\
H_{\mathrm{PFK}} &> 0 \\
\left[\frac{\kappa + H_{\mathrm{PK}}(q+1) + \alpha_x(1+B)}{q} - H_{\mathrm{PFK}}\right]&\left[\frac{(1+B)\kappa + H_{\mathrm{PK}}(q+1)}{q - \frac{\kappa}{\eta_x}} - H_{\mathrm{PFK}}\right] > \frac{\kappa}{q(q-\frac{\kappa}{\eta_x})}H_{\mathrm{PFK}}\,,
\end{aligned} \tag{9}$$

where

$$\begin{aligned}
H_{\mathrm{PFK}} &= -\alpha_f\frac{\bar{y}}{V_y} = -\frac{\partial f}{\partial y}(\bar{y})\frac{\bar{y}}{f(\bar{y})} \\
H_{\mathrm{PK}} &= -\alpha_w\bar{m}\frac{\bar{y}}{V_y} = -\frac{\partial w}{\partial y}(\bar{y})\frac{\bar{y}}{w(\bar{y})} \\
\kappa &= \frac{\bar{y}}{\bar{m}}, \quad \eta_y = \frac{\bar{y}}{V}\alpha_y, \quad \eta_x = \frac{\bar{y}}{V}\alpha_x\,.
\end{aligned}$$

We can check special cases of the general stability conditions by taking limit cases of the buffering speed b_x. As $b_x \to \infty$, the stability conditions are

$$0 < H_{\mathrm{PFK}} < \frac{(1+B)\kappa + H_{\mathrm{PK}}(q+1)}{q}\,,$$

which is identical to the 'rapid' buffering case. As $b_x \to 0$, the stability conditions are

$$0 < H_{\mathrm{PFK}} < \frac{\kappa + H_{\mathrm{PK}}(q+1)}{q},$$

which is equivalent to the case without buffering.

S2.3 Regulation of Buffered Glycolysis for Rapid Buffering and General Feedback

In this section, we analyze glycolysis with general feedback forms and rapid buffering. We study the fundamental constraints on glycolytic feedback regulation due to the the autocatalysis of ATP, and show how buffering relaxes these constraints.

We next look at the case of general feedback by studying fundamental constraints on feedback due to poles and zeros in the open loop system [10]. Taking the linearized model in Equation (4) and transforming to the frequency domain, we obtain

$$\begin{aligned} sM &= -wM + (\alpha_{f0} - C_h - \alpha_w \bar{m})Y \\ (1+B)sY &= (q+1)wM - (q(\alpha_{f0} - C_h) - (q+1)\alpha_w \bar{m})Y - V_y D_y \,, \end{aligned}$$

where $\alpha_f = \alpha_{f0} - C_h$ and $w = w(\bar{y})$. Rearranging gives us

$$\begin{aligned} (s+w)M &= (\alpha_{f0} - C_h - \alpha_w \bar{m})Y \\ ((1+B)s + q(\alpha_{f0} - C_h) - (q+1)\alpha_w \bar{m})Y &= (q+1)wM - V_y D_y \,. \end{aligned}$$

Further substitution gives us

$$((1+B)s + q(\alpha_{f0} - C_h) - (q+1)\alpha_w \bar{m})Y = (q+1)\frac{w}{s+w}(\alpha_{f0} - C_h - \alpha_w \bar{m})Y - V_y D_y \,,$$

and further rearrangement yields

$$\frac{Y}{D_y} = \frac{-V_y(s+w)}{(1+B)s^2 + [(1+B)w + q(\alpha_{f0} - C_h) - (q+1)\alpha_w \bar{m}]s - w(\alpha_{f0} - C_h)} \,.$$

Following [3], we set the weighted sensitvity function $Y/D_y = WS(s) = W(s)S(s)$ to be the classical weighted sensitivity function, where the weighting

$$W(s) = \frac{-V_y(s+w)}{s^2 + [w + q\alpha_{f0} - (q+1)\alpha_w \bar{m}]s - w\alpha_{f0}}$$

is the transfer function without PFK feedback or buffering, and the classical sensitivity function is

$$S(s) = \frac{s^2 + [w + q\alpha_{f0} - (q+1)\alpha_w \bar{m}]s - w\alpha_{f0}}{(1+B)s^2 + [(1+B)w + q(\alpha_{f0} - C_h) - (q+1)\alpha_w \bar{m}]s - w(\alpha_{f0} - C_h)} \,.$$

The sensitivity function can be rewritten as

$$\begin{aligned} S(s) &= \frac{s^2 + [w + q\alpha_{f0} - (q+1)\alpha_w \bar{m}]s - w\alpha_{f0}}{(1+B)s^2 + [(1+B)w + q(\alpha_{f0} - C_h) - (q+1)\alpha_w \bar{m}]s - w(\alpha_{f0} - C_h)} \\ &= \frac{s^2 + [w + q\alpha_{f0} - (q+1)\alpha_w \bar{m}]s - w\alpha_{f0}}{s^2 + [w + q\alpha_{f0} - (q+1)\alpha_w \bar{m}]s - w\alpha_{f0} + [Bs^2 + Bws - C_h qs + wC_h]} \\ &= \frac{1}{1 + \frac{Bs^2 + Bws - hqs + wh}{s^2 + [w + q\alpha_{f0} - (q+1)\alpha_w \bar{m}]s - w\alpha_{f0}}} \\ &= \frac{1}{1 + L(s)} \,, \end{aligned}$$

where

$$L(s) = \frac{Bs(s+w) + C_h(w - qs)}{s^2 + [w + q\alpha_{f0} - (q+1)\alpha_w \bar{m}]s - w\alpha_{f0}}$$

is the classical loop transfer function.

The classical loop transfer function is composed of two components corresponding the feedback and buffering, such that $L = L_B + L_H$, where

$$L_B = \frac{Bs(s+w)}{s^2 + [w + q\alpha_{f0} - (q+1)\alpha_w \bar{m}]s - w\alpha_{f0}}$$
$$L_H = \frac{C_h(w - qs)}{s^2 + [w + q\alpha_{f0} - (q+1)\alpha_w \bar{m}]s - w\alpha_{f0}}\,.$$

In [3], it was shown that the right-half plane (RHP) poles and zeros of the classical loop function fundamentally limits the regulation of glycolysis. It can be seen that PFK feedback is associated with a RHP zero at $z = w/q$. However, buffering is associated with a left-half plane (LHP) pole at $z = -w$, and so is not subject to the same fundamental constraints.

For proportional feedback, L has zeros at

$$Bs^2 + (Bw - qC_h)s + C_h w = 0\,,$$

which has solutions

$$z = \frac{-(Bw - qC_h) \pm \sqrt{(Bw - qC_h)^2 - 4BC_h}}{2B}\,,$$

meaning that the zeros are in the LHP if

$$C_h < \frac{q}{w} B\,.$$

If this case holds, there are no fundamental constraints on feedback due to RHP zeros.

Biologically, the RHP zero corresponds to the initial drop in ATP due to the investment stage of glycolysis, during which the ATP concentration initially decreases. The shifting of the zero from the RHP to the LHP corresponds to the buffer supplying the initial ATP investment to PFK.

We next assume that feedback may take any stable, causal form. $L(s)$ has zeros at

$$C_h(s)(w - qs) + Bs(s + w) = 0\,.$$

We can write

$$C_h(s) = h\frac{(s - z_1)\dots(s - z_m)}{(s - p_1)\dots(s - p_n)}\,,$$

where $m \leq n$, and so

$$s(s+w)(s-p_1)\dots(s-p_n) - \frac{qh}{B}(s-z_1)\dots(s-z_m)\left(s - \frac{w}{q}\right) = 0\,. \tag{10}$$

Equation (10) is a 'reverse' root locus problem if qh/B is treated as the gain, noting that here we are using the method to study the open-loop zeros rather than the closed-loop poles. The zeros of $L(s)$ start at 0, w, and the poles of the feedback. As qh/B is increased from zero, the zeros of $L(s)$ are all in the LHP, noting that the zero starting at $z = 0$ moves to the left (left of an even number of poles/zeros on the axis for 'reverse' root locus). Thus, for small qh/B, $L(s)$ has no RHP zeros. Or, in other words, the fundamental limits associated with RHP zeros are removed for a sufficiently large buffering equilibrium B.

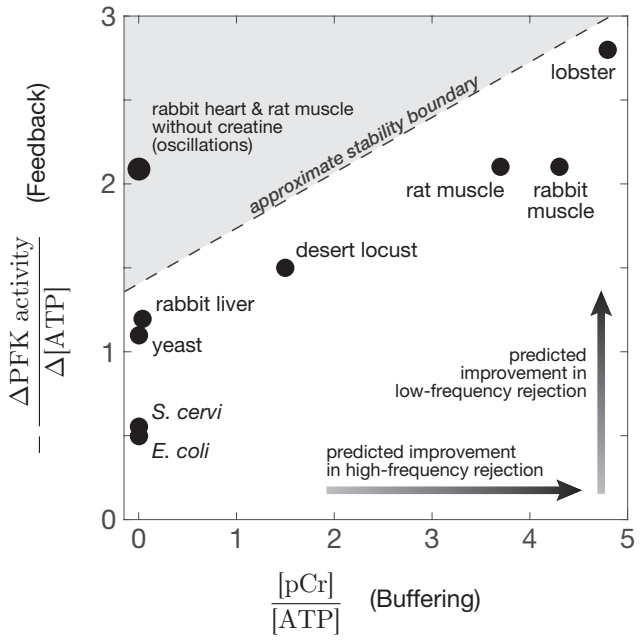


Figure S2.2: **Glycolytic Feedback vs Creatine Phosphate Buffering of ATP in Different Species** Using the ratios of normalized $-\Delta$PFK activity/Δ[ATP] and [pCr]/[ATP] as proxies for feedback gain and buffering ratio, respectively, we find empirical, cross-species support for a correlation between glycolytic feedback via PFK and ATP buffering by pCr. The shaded area in the figure corresponds to the unstable region, where the stability boundary is roughly and qualitatively estimated for illustrative purposes. This correlation, together with the theoretical in this study, and previously observed experimental cases of glycolytic oscillations induced by the removal of pCr, suggest that buffering enables higher-gain glycolytic feedback.

S2.4 Discussion: Comparison to Experimental Data

The following section compiles published experimental data for glycolytic feedback vs buffering within several different organisms. The published data shows a positive trend in feedback gain vs buffering equilibrium ratio. This trend, along with observed cases of oscillations that occur when buffering is removed, supports the notion of a critical feedback gain that is dependent upon buffering, as presented in the last section.

Motivated by the mathematical analysis, we investigated for an empirical relationship between glycolytic feedback via PFK and ATP buffering by pCr. Specifically, we compared proxies for the feedback gain, H_{PFK}, and the buffering equilibrium ratio, B, of different species. The feedback gain from ATP concentration to PFK activity served as a proxy for H_{PFK}, while the steady-state ratio $\bar{B} = [\text{pCr}]/[\text{ATP}]$ served as a proxy for the buffering equilibrium ratio B.

The feedback gain was estimated using

$$H_{\text{PFK}} = -\frac{\bar{y}}{f(\bar{y})}\frac{\Delta f}{\Delta y}, \tag{11}$$

where $\bar{y}$ is the nominal ATP concentration, $f(\bar{y})$ is the nominal PFK activity, and $\Delta f/\Delta y$ is the slope of PFK activity to ATP concentration at the nominal point. Experimental values for these three quantities were determined from literature, directly from plots of ATP concentration

vs PFK activity. Nominal values of ATP concentration and PFK activity were chosen at half maximum PFK activity, while the slope was estimated graphically at this same point. Lines of best fit were used to estimate the slope when available. The point of half maximum PFK activity was selected to estimate the maximum slope, which is the point most likely to cause instability. Using the point of half maximum PFK activity allowed a consistent approach across all data sets.

The data values that were selected from literature are presented in the table below and plotted in Figure S2.2 (a reproduction of Figure 8 in the main text). In the case of multiple sources, we plotted the first source listed in the table.

	normalized $\frac{-\Delta\text{PFK activity}}{\Delta[ATP]}$	Figure in Ref.	$\frac{[pCr]}{[ATP]}$ *
Rat Muscle	2.1 (avg.) [2]	Fig. 4	3.7 [1], 3.5 (avg.) [7]
Rabbit Muscle	2.1 [8], 2.4 [5]	Fig. 2, Fig. 4	4.3 [11]
Rabbit Liver	1.2 [5]	Fig. 4	small [4]
Desert Locust	1.5 (avg.) 1.3-1.7 (range) [15]	Fig. 3	1.5 [1]
Lobster Muscle	2.9 (avg.), 1.6-4.1(range) **[12]	Fig. 2	4.8 [1]
Yeast	1.1 [6]	Fig. 5	0
E. Coli	0.5 [17]	Fig 6A	0
Setaria cervi	0.55 [9]	Fig. 4	0

* alternatively arginine phosphate instead of pCr

** the feedback gain has the range $2 - 4.1$ using the local maximum slope, rather than the half activity point

For further support of the results, we also used data from published studies that have observed glycolytic oscillations after the removal of creatine phosphate: *in vitro*, in cell-free extracts of rat skeletal muscle [14, 13], and *in vivo*, in rabbit ventricular myocytes (when aerobic metabolism is also removed) [16]. These cases show that removal of ATP buffering can lead to feedback instability.

The stability boundary in Figure S2.2 (a reproduction of Figure 8 in the main text) is a qualitative approximation that does not take into account q or H_{PK} in Equation (7). It is included for illustrative purposes to highlight that the removal of buffering can lead to instability. We have, in the absence of experimental data, approximated the feedback gain in rabbit ventricular myocytes to be equal to that in rabbit skeletal myocytes, since both have predominantly the same PFK isoform.

References

[1] I. Beis and E. A. Newholme. The contents of adenine nucleotides, phosphagens and some glycolytic intermediates in resting muscles from vertebrates and invertebrates. *J. Biochem.*, 152(1):23–32, 1975.

[2] L. Bosca, J. J. Aragon, and A. Sols. Modulation of muscle phosphofructokinase at physiological concentration of enzyme. *J. Biol. Chem.*, 260(4):2100–2107, 1985.

[3] F. Chandra, G. Buzi, and J. C. Doyle. Glycolytic oscillations and limits on robust efficiency. *Science*, 333(8):187–192, 2011.

[4] A. H. Ennor and H. Rosenburg. The determination and distribution of phosphocreatine in animal tissues. *Biochem J.*, 51(5):606–610, 1951.

[5] R.G. Kemp. Rabbit liver phosphofructokinase: Comparison of some properties with those of muscle phosphofructokinase. *J. Biol. Chem.*, 246(1):245–252, 1970.

[6] G. Kopperschlager, R. Freyer, W. Diezel, and E. Hofman. Some kinetic and molecular properties of yeast phosphofructokinase. *FEBS Lett.*, 1(3):137–141, 1968.

[7] M.J. Kushmerick, T.S. Moerland, and R.W. Wiseman. Mammalian skeletal muscle fibers distinguished by contents of phosphocreatine, ATP, and Pi. *Proc. Natl. Acad. Sci. U.S.A.*, 89(16):7521–7525, 1992.

[8] D. W. Pettigrew and C. Friedens. Rabbit muscle phosphofructokinase: A model for regulatory kinetic behaviour. *J. Biol. Chem.*, 254(6):1896–1901, 1978.

[9] B. Sharma. Kinetic characterisation of phosphofructokinase purified from *Setaria cervi*: A bovine filarial parasite. *Enzyme Res.*, 2011:939472, 2011.

[10] S. Skogestad and I. Postlethwaite. *Multivariable Feedback Control: Analysis and Design*. Wiley, Chichester, 2005.

[11] K. B. Storey and P. W. Hochachka. Activation of muscle glycolysis: A role for creatine phosphate in phosphofructokinase regulation. *FEBS Lett.*, 46(1):337–339, 1974.

[12] P. H. Sugden and E. A. Newholme. The effects of ammonium, inorganic phosphate and potassium ions on the activity of phosphofructokinases from muscle and nervous tissues of vertebrates and invertebrates. *Biochem. J*, 150(1):113–122, 1975.

[13] K. Tornheim, V. Andre, and V. Schultz. Modulation by citrate of glycolytic oscillations in skeletal muscle extracts. *J. Biol. Chem.*, 266(24):15675–15678, 1991.

[14] K. Tornheim and J.M. Lowenstein. The purine nucleotide cycle: III. oscillations in metabolite concentrations during the operation of the cycle in muscle extract. *J. Biol. Chem.*, 248(8):2670–2677, 1973.

[15] R. Walker and E. Bailey. A comparison of the properties of the phosphofructokinases of the fat body and flight muscle of the adult male desert locust. *Biochem. J.*, 111(3):365–369, 1969.

[16] J-H. Yang, L. Yang, Z. Qu, and J. N. Weiss. Glycolytic oscillations in isolated rabbit ventricular myocytes. *J. Biol. Chem.*, 283(52):36231–36327, 2008.

[17] R-L. Zheng and R. G. Kemp. The mechanism of ATP inhibition of wild type and mutant phosphofructo-1-kinase from *Escherichia coli*. *J. Biol. Chem.*, 267(33):23640–23645, 1992.